MOLECULAR AND CELLULAR BIOLOGY, Mar. 1998, p. 1190–1200 Vol. 18, No. 3
0270-7306/98/$04.00+0

The *Saccharomyces cerevisiae RAD9* Checkpoint Reduces the DNA Damage-Associated Stimulation of Directed Translocations

MICHAEL FASULLO,[1,2]* THOMAS BENNETT,[2] PETER AHCHING,[1] AND JOE KOUDELIK[2]

Department of Biochemistry and Molecular Biology, The Albany Medical College, Albany, New York 12208-3479,[1] and Department of Radiotherapy, Loyola University Medical Center, Maywood, Illinois 60153[2]

Received 6 October 1997/Returned for modification 11 November 1997/Accepted 26 November 1997

Genetic instability in the *Saccharomyces cerevisiae rad9* mutant correlates with failure to arrest the cell cycle in response to DNA damage. We quantitated the DNA damage-associated stimulation of directed translocations in *RAD9*$^+$ and *rad9* mutants. Directed translocations were generated by selecting for His$^+$ prototrophs that result from homologous, mitotic recombination between two truncated *his3* genes, *GAL1::his3-Δ5′* and *trp1::his3-Δ3′::HOcs*. Compared to *RAD9*$^+$ strains, the *rad9* mutant exhibits a 5-fold higher rate of spontaneous, mitotic recombination and a greater than 10-fold increase in the number of UV- and X-ray-stimulated His$^+$ recombinants that contain translocations. The higher level of recombination in *rad9* mutants correlated with the appearance of nonreciprocal translocations and additional karyotypic changes, indicating that genomic instability also occurred among non-*his3* sequences. Both enhanced spontaneous recombination and DNA damage-associated recombination are dependent on *RAD1*, a gene involved in DNA excision repair. The hyperrecombinational phenotype of the *rad9* mutant was correlated with a deficiency in cell cycle arrest at the G_2-M checkpoint by demonstrating that if *rad9* mutants were arrested in G_2 before irradiation, the numbers both of UV- and γ-ray-stimulated recombinants were reduced. The importance of G_2 arrest in DNA damage-induced sister chromatid exchange (SCE) was evident by a 10-fold reduction in HO endonuclease-induced SCE and no detectable X-ray stimulation of SCE in a *rad9* mutant. We suggest that one mechanism by which the *RAD9*-mediated G_2-M checkpoint may reduce the frequency of DNA damage-induced translocations is by channeling the repair of double-strand breaks into SCE.

It has been postulated that DNA damage-induced cell cycle arrest at cell cycle checkpoints maintains genomic stability by allowing time for DNA repair prior to the replication or division of damaged chromatids (67, 68). Consistent with this idea, mutations in genes controlling cell cycle arrest at the G_1-S checkpoint and G_2-M checkpoint confer enhanced genetic instability. For example, p53 mutations, which confer deficiencies in the G_1-S checkpoint, are correlated with enhanced spontaneous and UV-stimulated amplification of *CAD* genes (35, 73). Cells cultured from patients with ataxia telangiectasia that are deficient in cell cycle arrest at both the G_1-S and G_2-M cell cycle checkpoints (7, 49) also exhibit higher frequencies of chromosomal rearrangements, including translocations (37) and deletions (38), and chromosome end-to-end joining (41).

In *Saccharomyces cerevisiae*, DNA-damaging agents stimulate mitotic, homologous recombination and induce cell cycle arrest at cell cycle checkpoints (31, 59). For example, DNA damage-associated recombination between *his3* fragments positioned at predetermined loci can result in chromosomal rearrangements, including translocations (18, 19), duplications (16), and deletions (54). HO endonuclease-generated double-strand breaks (DSBs) stimulate ectopic gene conversion between Ty1 elements and deletions between delta sequences (42). Because one DSB is sufficient to trigger *RAD9*-mediated cell cycle arrest at the G_2-M cell cycle checkpoint (8, 50), we asked whether cell cycle arrest at specific cell cycle checkpoints may channel recombinogenic DNA lesions into homologous recombination pathways that minimize genomic instability.

Recombinational repair of DSBs by sister chromatid exchange (SCE) may minimize genomic instability. Since resistance to ionizing radiation is greater in the G_2 phase of the cell cycle than in the G_1 phase in yeast (10, 11), it seems possible that sister chromatids are preferred substrates for the repair of DSBs by homologous recombination. Using a yeast strain containing tandemly repeated fragments of the *ade3* gene, Kadyk and Hartwell (27) found that X-ray-stimulated SCE is enhanced when cells are pretreated with the drug methyl benzimidazole-2-yl-carbamate, an agent that arrests cells in G_2. They concluded that X-ray-induced lesions are preferentially repaired via homologous recombination between sister chromatids rather than recombination between homologs. We speculate that in cell cycle mutants defective in arrest at the G_2-M checkpoint, unrepaired chromatids are more likely to be inherited in daughter cells and to increase the frequencies of some mitotic recombination events.

The *S. cerevisiae rad9* mutant (32), which is defective in cell cycle arrest at the G_1 (58, 59) and G_2 (67, 70) checkpoints, is hypersensitive to DNA-damaging agents including UV and ionizing radiation and exhibits higher levels of chromosome loss than *RAD9*$^+$ cells (69). However, no mitotic recombination phenotype has been established for the *rad9* mutant. *rad9* mutants do not exhibit higher levels of spontaneous, allelic recombination (69) or higher levels of spontaneous, intrachromatid deletions (53). In addition, the mitotic rate of spontaneous SCE is unchanged in *rad9* mutants (44). These previous studies did not analyze recombination events between nonhomologous chromosomes (ectopic recombination) that result in

* Corresponding author. Present address: Department of Biochemistry and Molecular Biology, The Albany Medical College, 47 New Scotland Ave., Albany, NY 12208-3479. Phone: (518) 262-6651. Fax: (518) 262-5689. E-mail: mfasullo@ccgateway.amc.edu.

TABLE 1. Yeast strains used in this study

Lab name	Genotype	Source
YA102	*MAT***a** *ura3-52 his3-Δ200 ade2-101 lys2-801 trp1-Δ1 gal3*$^-$	M. Carlson
YA148	*MAT***a** *ura3-52 his3-Δ200 ade2-101 lys2-801 leu2-Δ1 trp1-Δ63 Δcup1::ura3*	C. Guthrie
YB109	*MATα ura3-52 his3-Δ200 ade2-101 trp1-Δ1 gal3*$^-$ *leu2-3,112 GAL1::his3-Δ5′ trp1::his3-Δ3′::HOcs lys2*$^-$ (leaky)	This laboratory
YB110	YB109 × YA102	This laboratory
YB119	*MATα ura3-52 his3-Δ200 ade2-101 lys2-801 trp1-289 leu2-3,112 GAL1::his3-Δ5′*	This laboratory
YB130	*MATα ura3-52 his3-Δ200 ade2-101 trp1-Δ1 gal3*$^-$ *leu2-3,112 GAL1::his3-Δ5′ trp1::his3-Δ3′::HOcs lys2*$^-$ (leaky) *rad9::URA3*	*rad9* disruption in YB109
YB131	*MATα ura3-52 his3-Δ200 ade2-101 trp1-Δ1 gal3*$^-$ *leu2-3,112 GAL1::his3-Δ5′ trp1::his3-Δ3′::HOcs lys2*$^-$ (leaky) *rad9::LEU2*	*rad9* disruption in YB109
YB132	*MAT***a** *ura3-52 his3-Δ200 ade2-101 lys2-801 trp1-Δ1 rad9::URA3*	*rad9* disruption in YA102
YB133	*MAT***a** *ura3-52 his3-Δ200 ade2-101 lys2-801 leu2-Δ1 trp1-Δ63 Δcup1::ura3 rad9::LEU2*	*rad9* disruption in YA148
YB134	YB130 × YB132	This laboratory
YB135	YB131 × YB133	This laboratory
YB136	*MATα ura3-52 his3-Δ200 ade2-101 trp1-Δ1 gal3*$^-$ *leu2-3,112 GAL1::his3-Δ5′ trp1::his3-Δ3′::HOcs lys2*$^-$ (leaky) *rad1::URA3*	*rad1* disruption in YB109
YB137	*MAT***a** *ura3-52 his3-Δ200 ade2-101 lys2-801 trp1-Δ1 rad1::URA3*	*rad1* disruption in YA102
YB138	YB136 × YB137	This laboratory
YB139	*MAT***a** *ura3-52 his3-Δ200 ade2-101 lys2-801 leu2-Δ1 trp1-Δ63 Δcup1::ura3 rad9::LEU2*	*rad9* and *rad1* disruptions in YA148
YB140	*MATα ura3-52 his3-Δ200 ade2-101 trp1-Δ1 gal3*$^-$ *leu2-3,112 GAL1::his3-Δ5′ trp1::his3-Δ3′::HOcs lys2*$^-$ (leaky) *rad1::URA3 rad9::LEU2*	*rad9* and *rad1* disruptions in YB109
YB141	YB139 × YB140	This laboratory
YB142	*MAT***a** *ura3-52 his3-Δ200 ade2-101 lys2-801 leu2-Δ1 trp1-Δ63 Δcup1::ura3 rad9::URA3*	*rad9* disruption in YA148
YB143	*MATα ura3-52 his3-Δ200 ade2-101 trp1-Δ1 gal3*$^-$ *leu2-3,112 GAL1::his3-Δ5′ trp1::his3-Δ3′::HOcs lys2* (leaky) *rad9::URA3 rad52-7::LEU2*	*rad9* and *rad52* disruptions in YB109
YB144	*MAT***a** *ura3-52 his3-Δ200 ade2-101 lys2-801 leu2-Δ1 trp1-Δ63 Δcup1::ura3 rad9::URA3 rad52-7::LEU2*	*rad9* and *rad52* disruptions in YA148
YB145	YB143 × YB144	This laboratory
YB146	*MAT***a** *ura3-52 his3-Δ200 ade2-101 lys2-801 trp1-Δ1 gal3*$^-$ *trp1::[his3-Δ3′::HOcs his3-Δ5′]*	SCE assay in YA102
YB147	*MAT***a** *ura3-52 his3-Δ200 ade2-101 lys2-801 trp1-Δ1 gal3*$^-$ *trp1::[his3-Δ3′::HOcs his3-Δ5′] rad9::URA3*	*rad9* disruption in YB146
YB148	YB109 × YA148	This laboratory
YB149	*MAT***a** *ura3-52 his3-Δ200 ade2-101 lys2-801 leu2-Δ1 trp1-Δ63 Δcup1::ura3 rad1::URA3*	*rad1* disruption in YA148
YB150	YB136 × YB149	This laboratory
YB151	YB130 × YA102	This laboratory
YB152	*MAT***a** *ura3-52 his3-Δ200 ade2-101 lys2-801 leu2-Δ1 trp1-Δ63 Δcup1::ura3 rad52-7::LEU2*	*rad52* disruption in YA148
YB153	*MATα ura3-52 his3-Δ200 ade2-101 trp1-Δ1 gal3*$^-$ *leu2-3,112 GAL1::his3-Δ5′ trp1::his3-Δ3′::HOcs lys2*$^-$ (leaky) *rad52-7::LEU2*	*rad52* disruption in YB109
YB154	YB152 × YB153	This laboratory

chromosomal rearrangements or the effect of DNA-damaging agents on recombination frequencies.

In this study, we measured the spontaneous rates and the DNA damage-associated stimulation of directed translocations in both *RAD9*$^+$ and *rad9* mutant yeast strains. Both spontaneous, mitotic recombination and DNA damage-associated recombination resulting in chromosomal translocations were higher in *rad9* mutants, whereas levels of DSB-stimulated SCE were lower in *rad9* mutants. We suggest that the *rad9* mutant represents a novel class of mitotic recombination mutants in yeast, resulting from lack of cell cycle checkpoint control.

MATERIALS AND METHODS

Media and yeast strains. Media for the culture of bacteria are described in reference 3. Standard media for the culture of yeast, SC (synthetic complete, dextrose), SC-Trp (SC lacking tryptophan), SC-His (SC lacking histidine), SD (synthetic dextrose), YP (yeast extract, peptone), YPD (YP, dextrose), and sporulation media are described by Sherman et al. (57). YPL medium contains YP with 2% lactate (pH 5.5), and YPGal medium contains YP medium with 2% galactose. Ura$^-$ isolates (5-fluoro-orotic acid resistant [FOA^r]) were selected on FOA medium (9). Yeast transformations were performed as described by Chen et al. (12).

Relevant yeast strains are listed in Table 1. Strains used to monitor translocations contain truncated *his3* genes and were derived from YNN287 (16, 18). In this study, the *trp1::his3-Δ3′* gene fragment was replaced with *trp1::his3-Δ3′::HOcs*, containing the recognition sequence for HO endonuclease (*HOcs*).

The *his3-Δ3′::HOcs* gene fragment (Fig. 1) was constructed as follows. First, *his3-Δ3′* was constructed by *Kpn*I digestion of pUC18*HIS3* to generate 0.8- and 3.6-kb restriction fragments; the 3.6-kb *Kpn*I restriction fragment was circularized by DNA ligation, resulting in a deletion of the *his3* sequences that encode the 11 carboxyl-terminal amino acids (62, 63). The *Eco*RI-*Bam*HI restriction fragment containing *his3-Δ3′* was subcloned into the *Eco*RI-*Bam*HI sites of YIp5 (51). By *Bam*HI and *Bst*YI digestion, the 117-bp *MAT***a** fragment (30) was obtained from a modified version of pRK113 (*Hin*cII site converted to a *Bam*HI site [this study]) and was subcloned into the *Bgl*II sites of *his3-Δ3′*, replacing the 60-bp *HIS3 Bgl*II fragment. The 117-bp *MAT***a** fragment contains the minimal 24 bp necessary for HO endonuclease digestion (40).

The *his3-Δ3′::HOcs* gene fragment was transplaced (51) at *trp1* by using plas-

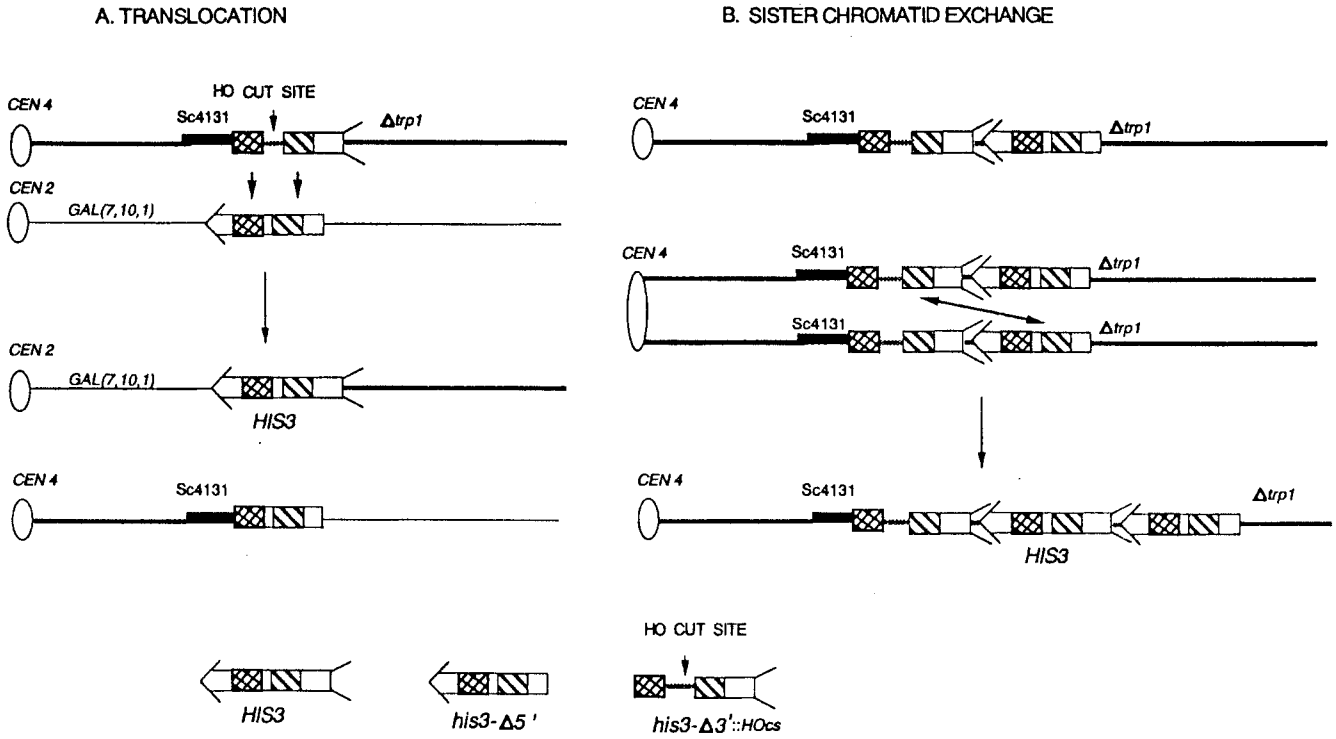

FIG. 1. Configurations of the *his3* recombinational substrates in strains used to generate reciprocal translocations (A) or SCE (B). For simplicity, the left arms of chromosomes II and IV are not shown. As shown at the bottom, an arrow without feathers represents *his3*-Δ*5′* and an arrow without an arrowhead represents *his3*-Δ*3′*. The recognition sequence for HO endonuclease, designated *HOcs*, is indicated by an arrow. Wild-type *HIS3* is depicted as an arrow with feathers and an arrowhead. The reciprocal product [*his3*-Δ*(5′,3′)*] lacks both arrowhead and feathers. Identical shadings within these truncated arrows indicate sequence similarity. The direction of the arrow is indicative of the polarity of the amino acid coding sequence. Heavy lines represent chromosome IV sequences, and ovals represent *CEN4*. Black boxes represent the 3.1-kb *Eco*RI fragment (Sc4131). Recombination between *his3* substrates generates the reciprocal translocation, *CEN2*::IV and *CEN4*::II, as shown at the bottom. (A) Strain construction in which *his3*-Δ*3′::HOcs* is transplaced in the genome at the *trp1* locus. (B) The *his3* substrates for the SCE assay after DNA replication of the chromatid (G_2). The product of unequal recombination between the tandem *his3* fragments is also shown.

mid MFp101, in which the 3′ and 5′ ends of the *his3*-Δ*3′::HOcs* fragment are flanked by chromosomal sequences Sc4131 and Sc4124 that map immediately centromere proximal and centromere distal (61), respectively, to the 1.45-kb *Eco*RI *TRP1* fragment. MFp100 is similar to the previously described plasmid pNN275 (17) except that MFp100 contains the *his3*-Δ*3′::HOcs* gene fragment. To create MFp101, a 1.2-kb *Bam*HI-*Xho*I partial fragment of Sc4124 was subcloned into the *Bam*HI-*Sal*I sites of MFp100. Plasmid MFp101 was then introduced into the diploid strain YB121 by selecting for Ura^+ transformants. A FOA^r isolate containing both *trp1::his3*-Δ*3′::HOcs* and *GAL1::his3*-Δ*5′* was sporulated and dissected; YB109 (Table 1) is a meiotic segregant containing both recombination substrates. The transplacement also deletes the entire *TRP1* gene and *GAL3* promoter sequences (65).

Strains to monitor SCE contain the *his3* fragments in tandem at *trp1* as previously described (16) except there are no direct repeats that flank the *his3* fragments. They were made by first selecting Ura^+ transformants of YA102 that contained plasmid MFp102 at *trp1*. MFp102 contains the *his3*-Δ*5′* gene fragment at the *Bam*HI site in MFp101 in the same orientation as in pNN287 (16). We then identified a FOA^r isolate (YB146) that generated His^+ recombinants.

Two sets of isogenic diploid strains containing *rad1*, *rad9*, or *rad52* null mutations were made by one-step gene replacement (48). One set is isogenic to the Rad^+ YB110, a diploid cross of YA102 and YB109, and the other set is isogenic to YB148, a diploid cross of YB109 and YA148. YA102 is derived from S288c, while YA148 is derived from a non-S288c strain containing a *cup1* deletion that was subsequently twice backcrossed with an S288c background (34). The *rad9::URA3*, *rad9::LEU2*, *rad52::LEU2*, and *rad1::URA3* disruptions were obtained by introducing digested DNA from plasmids pTW039, pTW0301 (69), pSM20 (55), and pDH23 (24), respectively, and selecting for transformants with the appropriate prototrophy. Haploid mutants containing both *rad9* and *rad1* disruptions or *rad9* and *rad52* disruptions were made by first introducing the *rad9* disruption and then introducing either the *rad1* or *rad52* disruption. Diploid strains were made by crossing strains derived from YB109 with those derived from YA102 or YA148, which do not contain the recombination substrates. Diploids isogenic to YB110 include the *rad9* (YB134) and the *rad1* (YB138) mutants. Diploids isogenic to YB148 include the *rad9* (YB135) and *rad1* (YB149) mutants and the *rad9 rad1* (YB141) and *rad9 rad52* (YB145) double mutants. The UV or γ-ray sensitivities of all transformants were confirmed.

Determining rates of spontaneous recombination and numbers of DNA damage-associated recombinants. The rates of spontaneous, mitotic events that generate either SCE or translocations (Table 2) were determined by the method of the median (33), as executed by Esposito et al. (14), using 11 independent colonies for each rate calculation. At least three independent rate calculations were done for each strain, and the significance of the differences between strains was determined by the Mann-Whitney *U* test (74).

The number of His^+ recombinants stimulated by DNA-damaging agents was determined by subtracting the spontaneous frequency from the stimulated frequency and multiplying by 10^7, the approximate number of cells plated, as done previously (17, 18). At least three independent experiments were done for each DNA-damaging agent. The significance of the differences between *rad9* mutants and $RAD9^+$ strains was determined by using the two-tailed paired sample *t* test (74). Protocols used to test the recombinogenicity of methyl methanesulfonate (MMS), UV, and γ rays have been described elsewhere (18, 19). The X-ray radiation source was purchased from Rad Source, Inc. (Wheeling, Ill.), and the dose rate was 440 rads/min. For measuring stimulation of SCE, cells were preincubated for 30 min in YPD after treatment with the DNA-damaging agent, washed twice with sterile H_2O, and then plated on selective medium (SC-His). Statistical significance of the X-ray stimulation of SCE was determined by the nonparametric sign test (74).

To arrest cells at the G_2 phase of the cell cycle, cells were grown to an A_{600} of 0.5 to 1 in YPD, nocodazole (methyl-5-[2-thienylcarbonyl]-*H*-benzimidazole-2-yl-carbamate) (25) was added to a concentration of 15 μg/ml, and cells were incubated at 30°C for 3 h. Cell cycle arrest was confirmed by visualization of large budded dumbbell-shaped structures in the light microscope; more than 95% of the cells were arrested. Cells were washed three times in sterile H_2O prior to irradiation.

Induction of HO endonuclease. The *HO* gene under *GAL* control (26) contained on pGHOT-*GAL3* (present study) was introduced into both $RAD9^+$ and *rad9* strains by selecting for Trp^+ transformants. pGHOT-*GAL3* was constructed by subcloning the *Sma*I-*Sal*I 3.5-kb *GAL3* fragment obtained from pT13B (65) into the *Xho*I site in pGHOT (40). Trp^+ isolates were then cultured in liquid SC-Trp and diluted in YPL. At a density of 10^7 cells/ml, glucose or galactose was added to a final concentration of 2%, to either repress or induce, respectively, expression of HO endonuclease. After 2 h, cells were plated directly on SC-His

TABLE 2. Rates of spontaneous translocations for *rad9*, *rad52*, and *rad1* mutants and *RAD9*$^+$ strains

Genotype[a]	Strain	Avg rate[b] ± SD	Ratio[c]
Strains isogenic to YB148			
RAD9/RAD9	YB148	$(3.3 \pm 1.6) \times 10^{-8}$	1.0
rad9::LEU2/rad9::LEU2	YB135	$(1.7 \pm 0.7) \times 10^{-7}$	5.1
rad1::URA3/rad1::URA3	YB150	$(2.1 \pm 1.0) \times 10^{-8}$	0.7
rad9::LEU2/rad9::LEU2	YB141	$(5.7 \pm 1.5) \times 10^{-8}$	1.7
rad1::URA3/rad1::URA3			
rad52::LEU2/rad52::LEU2	YB154	$<1.0 \times 10^{-9}$	<0.01
rad9::URA3/rad9::URA3	YB145	$<1.0 \times 10^{-9}$	<0.01
rad52::LEU2/rad52::LEU2			
Strains isogenic to YB110			
RAD9/RAD9	YB110	$(4.4 \pm 2.3) \times 10^{-8}$	1.0
rad9::URA3/rad9::URA3	YB134	$(1.8 \pm 0.4) \times 10^{-7}$	4.1
rad9::URA3/RAD9$^+$	YB151	$(6.0 \pm 3.4) \times 10^{-8}$	1.4
rad1::URA3/rad1::URA3	YB138	$(5.2 \pm 0.7) \times 10^{-8}$	1.2

[a] For full genotypes, see Table 1.
[b] As calculated by the method of the median; $n = 3$.
[c] Rate of recombination in mutant/rate of recombination in *RAD9*$^+$.

medium to measure prototroph formation and on SC medium or YPD medium to measure viability. Colonies were replica plated onto SC-Trp and SC media to determine the percentage of cells containing pGHOT-*GAL3*. No stimulation of recombination was observed when glucose was added to repress HO endonuclease.

Chromosomal DNA gels. Undigested yeast chromosomal DNA (56) was resolved on contour-clamped homogeneous electric field (CHEF) gels, using 220 V (6 V/cm) for 26 h at a 90-s pulse time (13). Chromosomal DNA was transferred to nylon membranes after exposure to 60 mJ of UV radiation for Southern blot analysis (60).

Verification that His$^+$ recombinants result from unequal SCE. Mitotic unequal SCE results in His$^+$ recombinants that contain *HIS3* flanked by *his3*-Δ*5′* (*his3*-Δ*2619* [62]) and *his3*-Δ*3′* (16). Southern blot hybridization (60) was used to detect a 4.6-kb *Eco*RI-*Sal*I restriction fragment that contains this configuration of *his3* fragments. The presence of *HOcs* in His$^+$ recombinants was determined by PCR (3), using primer 5′GTTGCGGAAAGCTGAAACTA3′ that anneals to the *HOcs* and primer 5′GGATCCGCTGCACGGTCCTG3′ that anneals upstream of the *HIS3* promoter present on *his3*-Δ*3′::HOcs*.

RESULTS

rad9 mutants exhibit higher frequencies of chromosome loss (69), but no mitotic recombination phenotype has been described. We observed that spontaneous and DNA damage-associated translocation events were increased in *rad9* mutants relative to *RAD9*$^+$ strains and then addressed three questions. Is enhanced recombination dependent on *RAD1* and *RAD52*? Is enhanced recombination correlated to deficiencies in cell cycle arrest and in DSB-induced SCE? What types of chromosomal rearrangements are found in *rad9* mutants?

Recombination assays. To quantitate frequencies of either directed translocations or SCEs, we selected His$^+$ recombinants that result from mitotic recombination between two truncated *his3* fragments (16) (Fig. 2). Strains used to quanti-

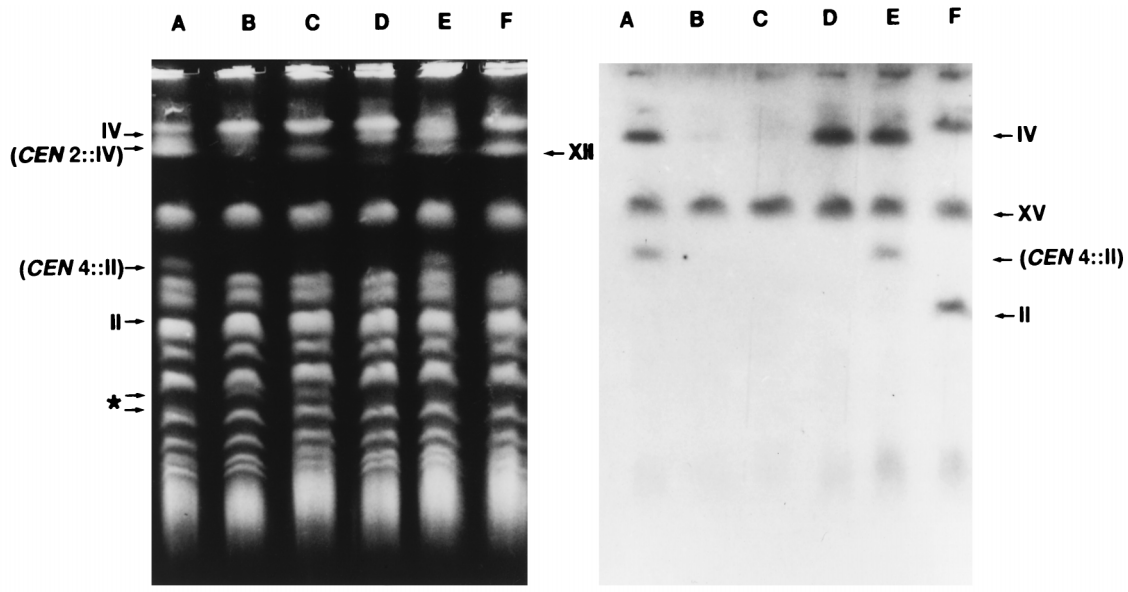

FIG. 2. Electrophoretic karyotypes of spontaneous and DNA damage-associated His$^+$ recombinants resulting from ectopic recombination of *GAL1::his3*-Δ*5′* and *trp1::his3*-Δ*3′::HOcs* in *rad9* mutant YB134. An ethidium bromide-stained CHEF gel is shown on the left, and a Southern blot probed with ^{32}P-labeled *HIS3* is shown on the right. Arrows point to the positions of translocations, and the asterisk indicates the position of additional chromosomal polymorphisms. Lanes: A, MMS-induced reciprocal translocation; B, DNA damage-induced His$^+$ recombinant in which *CEN2*::IV is mitotically unstable; C, spontaneous His$^+$ in which *CEN2*::IV is unstable; D, spontaneous nonreciprocal translocation; E, reciprocal translocation; F, His$^-$ YB134 (parental configuration).

TABLE 3. Stimulation of translocations by DNA-damaging agents in *RAD9*$^+$ and *rad9::URA3* diploids

Agent	Stimulation in *RAD9*$^+$ (YB110[a])			Stimulation in *rad9* (YB134[a])			Ratio[c]
	Concn or dose	Survival (%)	His$^+$/10^7 CFU[b]	Concn or dose	Survival (%)	His$^+$/10^7 CFU	
MMS	0.1%	94	59 ± 13	0.1%	81	246 ± 21	4.2
	10.5 mM			10.5 mM			
UV	150 J/m^2	94	98 ± 12	150 J/m^2	68	733 ± 183	7.5
	120 J/m^2	97	52 ± 12	120 J/m^2	67	563 ± 98	11
	60 J/m^2	98	38 ± 10	60 J/m^2	89	296 ± 57	7.8
γ rays	23.4 Kilorads	76	314 ± 44	23.4 Kilorads	21	984 ± 212	3.1
	15.6 Kilorads	79	192 ± 6	15.6 Kilorads	38	1,056 ± 197	5.5
	7.8 Kilorads	94	85 ± 5	7.8 Kilorads	76	587 ± 121	6.9
	3.9 Kilorads	100	31 ± 5	3.9 Kilorads	95	212 ± 45	6.8
X rays	2.2 Kilorads	88	9 ± 4	2.2 Kilorads	77	137 ± 37	15
	880 Rads	86	4 ± 4	880 Rads	89	43 ± 31	11

[a] For complete genotypes, see Table 1.
[b] (His$^+$ frequency with agent − His$^+$ spontaneous frequency) × 10^7; $n = 3$.
[c] (His$^+$/10^7 CFU for *rad9*)/(His$^+$/10^7 CFU for *RAD9*$^+$). Spontaneous frequency of YB110 = (6.2 ± 3.2) × 10^{-8} ($n = 33$); spontaneous frequency of YB134 = (6.9 ± 2.1) × 10^{-7} ($n = 33$).

tate numbers of translocations contain the *his3* fragments positioned on chromosomes II and IV (16, 17), while strains used to quantitate SCEs contain the truncated fragments of *his3* in tandem at the *trp1* locus. The *trp1::his3-Δ3′::HOcs* fragment was used to directly target HO endonuclease-induced DSBs. Diploid strains that monitor translocations contain one set of chromosome II and IV homologs that do not contain recombinational substrates.

Rates of spontaneous, mitotic recombination in *rad9* mutants. Isogenic haploid and diploid *rad9* mutant strains were made by one-step gene replacement (48) using either the *rad9::LEU2* or *rad9::URA3* disruption. Rates of spontaneous His$^+$ recombinants that contain translocations in both haploid and diploid strains increased, as measured by the method of the median (Table 2). The rate of mitotic recombination in *rad9::URA3* haploid strain YB130 increased significantly ($P < 0.05$) to 5.4 × 10^{-8} from the rate of 2 × 10^{-8} observed in *RAD9*$^+$ strain YB109. Rates of spontaneous mitotic recombination for both the *rad9::URA3* homozygous diploid strain (YB134) and the *rad9::LEU2* homozygous diploid strain (YB135) are four- and fivefold higher ($P < 0.05$) than the rates observed for the wild-type *RAD9*$^+$ homozygous diploids YB110 and YB148, respectively. There are no significant differences ($P > 0.5$) between the rates of recombination for the *RAD9*$^+$ strains YB110 and YB148 or between the rates of recombination for the *rad9* mutants YB134 and YB135. The rate of mitotic recombination in the *RAD9*$^+$ heterozygous diploid (YB151) is not significantly different ($P > 0.5$) from that in wild-type strain YB110. Thus, an enhanced rate of spontaneous recombination that generates translocations can be detected in diploid *rad9* mutants.

We also determined rates of spontaneous translocations for *rad1* and *rad52* single mutants and *rad9 rad1* and *rad9 rad52* double mutants to determine whether the excision repair pathway or the recombinational repair pathway contributed to the higher recombination observed in *rad9* mutants (Table 2). In comparison to the *RAD9*$^+$ strains (YB110 and YB148), there is no significant decrease ($P > 0.05$) in rates of translocations in *rad1* mutants. However, rates of translocations in the *rad9 rad1* mutant (YB141) are not significantly different ($P > 0.3$) from the level of the *RAD9*$^+$ strain (YB148). No recombinants were detected in either the *rad52* mutant (YB154) or the *rad9 rad52* mutant (YB145). Thus, higher rates of spontaneous translocations observed in *rad9* mutants are dependent on *RAD1* and *RAD52*.

DNA damage-associated stimulation of directed translocations in *rad9* mutants. Since the DNA lesions that initiate spontaneous recombination are unknown, we investigated whether the recombinogenicity of DNA-damaging agents that produce specific DNA lesions would increase in *rad9* mutants. UV, γ rays, and MMS, which are known to trigger cell cycle arrest at the G_2-M checkpoint, stimulate the formation of directed translocations in both haploid and diploid Rad$^+$ strains (19). Since the stimulation of translocations is greater in Rad$^+$ diploids than in Rad$^+$ haploids (19), the stimulation of translocations after exposure to UV, γ rays, or MMS was also quantitated for the diploid *rad9* mutant (YB134). Compared with the *RAD9*$^+$ diploid YB110 (Table 3), the greatest enhancement in the stimulation of translocations, 15-fold for X rays and 11-fold for UV, occurred after the diploid *rad9* mutant was exposed to intermediate levels of radiation. Although the peak in the numbers of stimulated His$^+$ recombinants in the *rad9* mutant occurred at higher levels of radiation exposure, the lower enhancement of recombination may result from the radiation sensitivity of the *rad9* mutant. The greater enhancement in the numbers of X-ray-stimulated translocations (15-fold) compared to γ-ray stimulated translocations (7-fold) may result from the higher dose rate (440 rads/min) of ionizing radiation delivered by the X-ray source. The stimulation of translocations by the alkylating agent MMS exhibited a significant ($P < 0.05$) fourfold increase in the *rad9* mutant. Thus, the

TABLE 4. γ-Ray stimulation of translocations in *rad* mutants of *S. cerevisiae*

Genotype[b]	Strain	Avg frequency[a] ± SD		
		7.8 Kilorads	15.6 Kilorads	23.4 Kilorads
RAD9/RAD9	YB148	61 ± 16	145 ± 45	242 ± 24
rad1/rad1	YB150	30 ± 10	49 ± 10	74 ± 30
rad9/rad9	YB135	429 ± 46	871 ± 70	781 ± 102
rad9/rad9 rad1/rad1	YB141	62 ± 39	228 ± 40	44 ± 36

[a] (Frequency of His$^+$ recombinants after irradiation − frequency of spontaneous His$^+$ recombinants) × 10^7; $n = 3$.
[b] For full genotypes, see Table 1. All strains are derived from YB148.

TABLE 5. Stimulation of translocations in *rad9* mutants when cells are pretreated with nocodazole

Treatment	Avg frequency[a] ± SD		Ratio[c]
	RAD9$^+$ (YB110[b])	*rad9* (YB134[b])	
UV (60 J/m^2)	38 ± 10	296 ± 57	7.8
Nocodazole + UV (60 J/m^2)	9 ± 2	33 ± 11	3.7
Fold reduction[d]	4.2	9.0	
γ rays (3.9 kilorads)	31 ± 5	212 ± 45	6.8
Nocodazole + γ rays (3.9 kilorads)	18 ± 2	41 ± 21	2.3
Fold reduction	1.7	5.2	
γ rays (7.8 kilorads)	85 ± 5	587 ± 121	6.9
Nocodazole + γ rays (7.8 kilorads)	42 ± 11	108 ± 56	2.6
Fold reduction	2	5.4	

[a] (Frequency of His$^+$ recombinants with agent − frequency of spontaneous His$^+$ recombinants) × 10^7; $n = 3$.
[b] For complete genotypes, see Table 1.
[c] Stimulated His$^+$ in *rad9*/stimulated His$^+$ in *RAD9* (see Table 3, footnote *c*).
[d] Agent/(nocodazole + agent).

recombinogenicity of DNA-damaging agents that create DNA base pair damage, DNA cross-links, or DNA strand breaks is enhanced in *rad9* mutants.

To determine whether the enhanced DNA damage-associated recombination observed in *rad9* mutants is dependent on *RAD1*, single and double mutants were made by one-step gene replacement. Similar to the *RAD9*$^+$ strain (YB148), the number of γ-ray-stimulated His$^+$ recombinants in the *rad1* mutant (YB150) increased in a dose-dependent manner but was ~3-fold less ($P < 0.05$). In comparison to the *rad9* mutant (YB135), the number of γ-ray-stimulated recombinants in the *rad1 rad9* double mutant (YB141) also peaked at 15.6 kilorads but was significantly reduced ($P < 0.05$) at all levels of radiation exposure (Table 4). The reduced number of stimulated recombinants in the *rad1 rad9* double mutant at 23.4 kilorads does not result from differences in radiation sensitivity, since the sensitivity of the *rad1 rad9* double mutant to ionizing radiation cannot be distinguished from the *rad9* single mutant at all indicated doses (data not shown). Thus, the enhanced level of γ-ray-stimulated translocations observed in *rad9* mutants is also dependent on *RAD1*.

The stimulation of translocations in cells treated with nocodazole before irradiation. To determine whether the increase in DNA damage-associated recombination was correlated with failure to arrest the cell cycle at the G_2-M checkpoint, both *RAD9*$^+$ and *rad9* mutant cells were prearrested at the G_2 phase with the microtubule inhibitor nocodazole before irradiation. As a control, we confirmed that the resistance to γ irradiation of the *rad9* cells increased to wild-type levels by using this protocol (data not shown), as previously shown (67). It thus seems plausible that if the cell cycle was arrested at the G_2 phase before irradiation, higher levels of DNA damage-associated translocations observed in the *rad9* mutant would be reduced. Pretreatment with nocodazole without subsequent irradiation did not affect recombination frequencies (data not shown). The stimulation of His$^+$ recombinants in the nocodazole-arrested cells after exposure to γ rays decreased in the *rad9* mutant at least fivefold, but the level of recombination in the wild-type cells was not significantly reduced ($P > 0.05$). The UV stimulation of translocations decreased in both the *RAD9* wild-type (YB110) and the *rad9* mutant (YB134) background (Table 5) when cells were pretreated with nocodazole, although the decrease in the level of recombination was greater in the *rad9* mutant (ninefold) than in the *RAD9* wild-type strain (fourfold). Thus, by prearresting cells at the G_2 phase, the radiation-associated stimulation of translocations is decreased in *rad9* mutants.

Stimulation of translocations by HO-induced DSBs in the *rad9* mutant. To determine whether the enhanced level of recombination observed in the *rad9* mutant is also observed for a single directed DSB, the pGHOT-*GAL3* plasmid, containing the galactose-inducible *HO* gene, was introduced into both diploid *RAD9*$^+$ and *rad9* strains. HO endonuclease digestion at *trp1::his3-Δ3′::HOcs* results in a DSB in which 117 bp of the centromere proximal end and ~300 bp of the centromere distal end are homologous to the *his3-Δ5′* fragment (Fig. 1). Because the number of CFU decreases after HO induction and the pGHOT plasmid is lost in 5 to 10% of the cells in nonselective growth conditions, frequencies of His$^+$ recombinants were quantitated per Trp$^+$ CFU before and after HO induction; His$^-$ cells that lost pGHOT-*GAL3* were thus excluded from the calculations. Since the *HO* gene is weakly expressed under nonrepressing growth conditions, there was >5-fold increase in the recombination frequencies for the *rad9* mutant and the *RAD9*$^+$ strains, respectively, before galactose induc-

TABLE 6. Stimulation of translocations and SCE by HO-induced DSBs

Strain[a]	No. of expts	Avg viability after HO induction ± SD (%)[b]	Avg frequency of His$^+$ recombinants ± SD			Avg no. of stimulated His$^+$ recombinants/10^6 cells[f] ± SD
			Before HO induction, per Trp$^+$ CFU from YPL[c]	After HO induction		
				Per Trp$^+$ CFU from YPL[d]	Per Trp$^+$ CFU from YPGal[e]	
To monitor translocations						
RAD9$^+$ diploid (YB110)	8	89 ± 9	$(4.5 \pm 2.3) \times 10^{-6}$	$(1.6 \pm 0.2) \times 10^{-4}$	$(2.2 \pm 0.3) \times 10^{-4}$	201 ± 19
rad9 mutant (YB134)	3	75 ± 7	$(3.8 \pm 0.7) \times 10^{-6}$	$(1.8 \pm 0.1) \times 10^{-4}$	$(2.3 \pm 0.2) \times 10^{-4}$	173 ± 6
To monitor SCE						
RAD9$^+$ (YB146)	5	91 ± 13	$(7.5 \pm 6.0) \times 10^{-5}$	$(7.9 \pm 2.0) \times 10^{-4}$	$(8.6 \pm 2.3) \times 10^{-4}$	715 ± 163
rad9::URA3 (YB147)	4	77 ± 9	$(3.8 \pm 1.1) \times 10^{-5}$	$(7.1 \pm 1.8) \times 10^{-5}$	$(9.3 \pm 2.2) \times 10^{-5}$	35 ± 23

[a] For complete genotypes, see Table 1.
[b] (Trp$^+$ CFU after HO induction/Trp$^+$ CFU before HO induction) × 100.
[c] Number of His$^+$ recombinants before HO induction/number of Trp$^+$ cells at the time of HO induction.
[d] Number of His$^+$ recombinants after HO induction/number of Trp$^+$ cells at the time of HO induction.
[e] Number of His$^+$ recombinants after HO induction/viable Trp$^+$ cell after HO induction.
[f] Average (frequency of His$^+$ recombinants after HO induction − frequency of His$^+$ recombinants before HO induction) × 10^6.

TABLE 7. Electrophoretic karyotypes of His^+ recombinants containing translocations in *rad9* mutant and *RAD9*$^+$ strains

Strain	Chemical or agent	No. of His^+ recombinants containing indicated rearrangement(s)			
		Reciprocal translocation[a]	Reciprocal translocation and other[b]	Nonreciprocal translocation[c]	Nonreciprocal translocation and other
YB134 (*rad9*/*rad9*)	MMS	2	1	2	0
	UV	5	1	7	0
	γ rays	2	0	3	0
	Spontaneous	2	0	10	2
	Total	11	2	22	2
YB110 (*RAD9*/*RAD9*)	UV	16	0	0	0
	γ rays	16	0	0	0
	Spontaneous	16	0	0	0
	Total	48	0	0	0

[a] *CEN2*::IV and *CEN4*::II.
[b] "Other" includes polymorphism of chromosome VI and chromosomal band between chromosomes V and VIII (see Fig. 2).
[c] *CEN2*::IV.

tion of HO. There were no significant differences ($P > 0.05$) in the frequencies or number of HO endonuclease-stimulated His^+ recombinants between *RAD9*$^+$ and *rad9* mutant strains (Table 6). Thus, enhanced recombination was not observed for a single directed DSB. We speculate that the inability to detect elevated levels of translocation events results when both sister chromatids are digested at identical sites.

Nonreciprocal translocations and chromosomal polymorphisms are generated in *rad9* mutants. We compared the electrophoretic karyotypes of His^+ recombinants derived from the *RAD9*$^+$ strain (YB110) and the *rad9* mutant strain (YB134) to determine whether the same types of chromosomal rearrangements are generated in both strains (Fig. 2). We observed four classes of electrophoretic karyotypes for His^+ recombinants that differ from the parental His^+ karyotype (Table 7). These include (i) reciprocal translocations containing only *CEN4*::II and *CEN2*::IV, (ii) nonreciprocal translocations containing only *CEN2*::IV, and (iii) reciprocal or (iv) nonreciprocal translocations associated with other heterogeneous genomic rearrangements unrelated to homologous recombination between *his3* sequences. Nonreciprocal translocations containing only *CEN4*::II could not be selected on SC-His since *HIS3* is contained on *CEN2*::IV. Karyotypes were determined for 16 UV- and 16 γ-ray-stimulated His^+ recombinants that arose after 3 days on selective medium from the Rad^+ diploid YB110, and all of 32 stimulated recombinants contain reciprocal translocations. In contrast, the majority of both spontaneous and DNA damage-associated recombinants (24 of 37) obtained from the *rad9* mutant (YB134) contain nonreciprocal translocations and, less frequently, reciprocal translocations (13 of 37).

A few (4 of 37) His^+ recombinants obtained from the *rad9* mutant YB134 also contain additional chromosomal polymorphisms (Fig. 2) in association with translocations. They include a novel chromosome VI band and chromosome polymorphisms that map between chromosomes V and VIII (Fig. 2, lanes A to C). Southern blot analysis of a CHEF gel demonstrated that these novel polymorphisms do not contain significant sequence similarity to either *HIS3* (Fig. 2) or Sc4124, centromeric sequences from chromosome IV (data not shown). The recombination mechanism that generates these chromosomal polymorphisms must include an alternative mechanism other than recombination between *his3* fragments. Thus, the hyperrecombinational (hyper-Rec) phenotype associated with *rad9* may also be relevant to naturally occurring genomic sequences.

In two of the four His^+ recombinants containing chromosomal rearrangements besides the *CEN4*::II and the *CEN2*::IV translocations, the *CEN2*::IV translocation which contains *HIS3* was mitotically unstable. For both reciprocal and nonreciprocal translocations, the *CEN2*::IV translocation is lost infrequently (<1%) after 10 generations of growth on nonselective (YPD) medium, as indicated by the stability of the His^+ phenotype and the appearance of the translocation on CHEF gels. In the two His^+ recombinants containing additional chromosomal polymorphisms, *CEN2*::IV is lost frequently after 10 generations of growth on nonselective (YPD) medium, as is

TABLE 8. Stimulation of SCE by DNA-damaging agents in *RAD9*$^+$ and *rad9::URA3* mutant strains

Agent	Stimulation in *RAD9*$^+$ (YB146[a])			Stimulation in *rad9* (YB147[a])			Ratio[c]
	Concn or dose	Survival (%)	$His^+/10^7$ CFU[b]	Concn or dose	Survival (%)	$His^+/10^7$ CFU	
X rays	4.4 Kilorads	38	155 ± 85	4.4 Kilorads	24	<10	16
	2.2 Kilorads	61	20 ± 19	2.2 Kilorads	49	<10	2
	880 Rads	80	<10	880 Rads	61	<10	1
MMS	0.1%	63	1,097 ± 278	0.1%	40	828 ± 125	1.3
	10.5 mM			10.5 mM			
UV	60 J/m^2	55	554 ± 117	60 J/m^2	13	416 ± 154	1.3
	30 J/m^2	75	338 ± 44	30 J/m^2	38	208 ± 26	1.6

[a] For complete genotypes, see Table 1.
[b] (His^+ frequency with agent − His^+ spontaneous frequency) × 10^7; $n = 5$.
[c] ($His^+/10^7$ CFU for *RAD9*)/($His^+/10^7$ CFU for *rad9*). There is no significant difference ($P > 0.05$) between the X-ray stimulations of SCE for YB146 and YB147 strains after 2.2 kilorads and 880 rads. Spontaneous frequency of SCE in YB146 = (1.1 ± 0.2) × 10^{-5} ($n = 33$); spontaneous frequency of SCE in YB147 = (8.6 ± 1.1) × 10^{-6} ($n = 33$).

evident on CHEF gels (Fig. 2) and by the instability of the His^+ phenotype, which ranged from 381 (His^-) of 402 (total) CFU (95%) to 43 (His^-) of 1,001 (total) CFU (4%). Additional chromosomal rearrangements may have occurred to decrease the mitotic stability of *CEN2*::IV in these recombinants.

X-ray- and HO-induced SCE are decreased in *rad9* mutants. We hypothesize that the G_2-M checkpoint serves to arrest the cell cycle and allows for the repair of DNA damage present on sister chromatids. If this hypothesis is correct, *rad9* mutants should exhibit reduced stimulation of SCE after exposure to agents that create DSBs. To determine whether DSB-stimulated SCE differed in either *rad9* mutants or *RAD9*$^+$ strains, we made a novel strain (YB146) so that SCE could also be stimulated by targeted HO-induced DSBs (Fig. 1). SCE was monitored by selecting for His^+ prototrophs as previously described (16). A *rad9::URA3* congenic strain was made by one-step gene replacement. Rates of spontaneous SCE were 1.6×10^{-6} in a *RAD9*$^+$ strain (YB146) and 1.4×10^{-6} in an isogenic *rad9::URA3* (YB147) mutant.

RAD9$^+$ and *rad9* mutant strains were exposed to X rays, UV, and MMS to determine whether DNA damage-stimulated SCE was decreased in *rad9* mutants. X-ray exposure of *RAD9*$^+$ cells resulted in the stimulation of $\sim 150 \times 10^{-7}$ His^+ recombinants resulting from SCE (Table 8), which is significantly different from the nonirradiated control ($P < 0.05$). X-ray exposures greater than 4.4 kilorads did not stimulate more SCE. X-ray stimulation of SCE was not observed in the *rad9* mutant, and no statistically significant changes in recombination frequencies were observed ($P > 0.1$) (Table 8). UV and MMS stimulated SCE in either *RAD9*$^+$ or *rad9* strains; however, there are fewer MMS- and UV-stimulated recombinants in the *rad9* mutant ($P < 0.05$). Thus, SCE stimulation in *rad9* mutants depends on the DNA-damaging agent.

Since UV, X rays, and MMS generate a variety of DNA lesions that may stimulate SCE, we examined the role of a site-specific DSB in stimulating SCE. After introduction of pGHOT-*GAL3* into the *RAD9*$^+$ and *rad9* strains, the HO endonuclease was induced, and the HO-induced frequencies of His^+ recombinants and the percent survival after HO induction were determined (Table 6). Survival decreased from 91% in the *RAD9*$^+$ strain to 77% in the *rad9* mutant per number of cells containing pGHOT-*GAL3*. Whereas there was a 10-fold increase in the frequency of recombination after HO induction in *RAD9*$^+$ cells, there was no significant increase ($P > 0.1$) in recombination after HO induction in the *rad9* mutant. To verify that HO endonuclease was active in the *rad9* mutant, the efficiency of HO-induced mating-type switching was determined for both the *rad9* mutant (YB147) and the *RAD9*$^+$ strains. For both strains, ~50% of the cells that survived HO induction had also switched mating type.

HO-induced DSBs could theoretically stimulate both intrachromatid recombination and SCE. Unequal SCE was confirmed by Southern blot analysis as previously described (16). Since no replication origin is present in *HIS3*, there is a low probability that His^+ recombinants can result from intrachromatid recombination generating an extrachromosomal *HIS3* and reintegration of *HIS3*. Southern blot analysis demonstrated that seven of nine HO-induced His^+ recombinants from the *RAD9*$^+$ strain (YB148) resulted from SCE (16). Multiple rounds of unequal SCE might have occurred to generate the other two His^+ recombinants, as suggested by the presence of larger restriction fragments that contain *his3* fragments (data not shown). Among HO-induced His^+ recombinants from the *rad9* mutant, six of eight resulted from unequal SCE and two His^+ recombinants may have resulted from multiple rounds of exchange. PCR analysis revealed that among HO-induced recombinants, one of nine His^+ recombinants from the *RAD9*$^+$ strain and four of eight His^+ recombinants from the *rad9* mutant still contained an *HOcs* at *his3-Δ3′*, whereas 10 of 10 spontaneous His^+ recombinants from the *rad9* mutant contain the *HOcs* at *his3-Δ3′*. Thus, DSB-induced SCE occurred in both *RAD9*$^+$ and *rad9* mutant strains but was less frequent in the *rad9* mutant.

DISCUSSION

The *rad9* mutant of *S. cerevisiae* exhibits pleiotropic phenotypes, including radiation sensitivity and higher frequencies of chromosome loss, that are attributed to lack of cell cycle arrest at the G_2-M cell cycle checkpoint (67, 69, 70). In this study, the genetic instability phenotype of *rad9* was extended to include the following two novel recombination phenotypes: (i) a significant increase in both the spontaneous and DNA damage-associated frequencies of directed translocations and (ii) a decrease in the DSB-induced frequencies of SCE. Three major conclusions can be inferred from experiments to characterize these novel phenotypes. First, the higher level of recombination induced by the DNA-damaging agents in the *rad9* mutant results from failure to arrest the cell cycle at the G_2-M checkpoint. Second, recombinational pathways in *rad9* mutants that generate higher levels of translocation events involve both *RAD1* and *RAD52*. Third, the *rad9*-enhanced recombination is not limited to recombination between *his3* sequences.

These conclusions were based on quantitating directed translocation events in diploid strains. Although elevated rates of spontaneous translocations were also observed for a haploid *rad9* mutant, in comparison to *RAD9*$^+$ strains, there is more stimulation for diploid *rad9* mutants. Higher levels of translocation events in *rad9* diploids may be ascribed to higher frequencies of chromosome loss exhibited by *rad9* mutants, which might reduce the number of viable recombinants in haploid cells (69).

Two possible explanations for the *rad9* recombination phenotypes are (i) failure to arrest the cell cycle at the G_2-M checkpoint and (ii) one or more errors in DNA metabolism or DNA damage-induced gene expression in *rad9* mutants. The first explanation implies that recombination phenotypes result from failure to repair recombinogenic lesions prior to the segregation of sister chromatids; specific timing of gene conversion in G_1 and crossovers in G_2 has been previously suggested (15, 23, 47). The second explanation implies that recombination is stimulated by more recombinogenic lesions or by a bias in processing of recombination intermediates toward reciprocal exchange. Pleiotropic phenotypes of *rad9* mutants include a deficiency in the DNA damage inducibility of genes such as *RAD51* (1), which is involved in DSB repair and gene conversion (45), and the accumulation of single-strand DNA gaps resulting from expression of the putative Rad17 nuclease (36).

Deficient cell cycle arrest at G_2 leads to more translocation events in *rad9* mutants. Our results support the hypothesis that higher numbers of DNA damage-associated translocations result from altered timing of recombinational repair and that the *RAD9*-dependent checkpoint is triggered by DNA damage (67). First, there is a twofold-greater difference between *rad9* and *RAD9*$^+$ strains when numbers of radiation-induced translocations are compared than when rates of spontaneous translocations are compared. Second, the elevated DNA damage-associated recombination in *rad9* mutants can be suppressed when cells are temporarily arrested in G_2-M phase by a microtubule inhibitor prior to irradiation. This implies that the G_2 checkpoint serves to channel DNA damage into either a nonrecombinogenic repair pathway or a recombination pathway

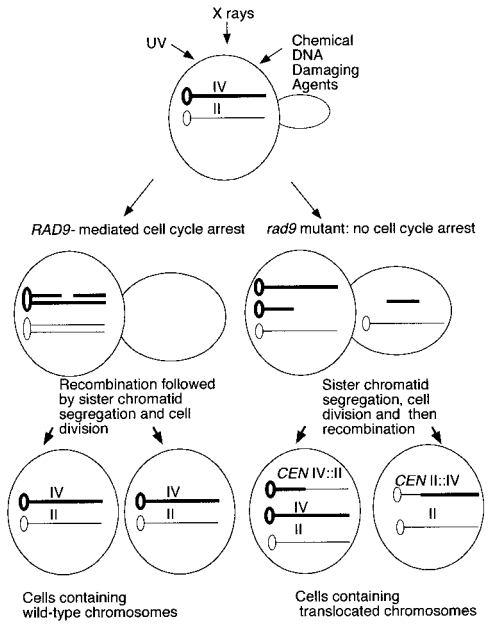

FIG. 3. Diagram of the generation of chromosomal rearrangements in *rad9* mutants. Large circles represent the mother cell, and large ovals emerging from the mother cell represent the daughter bud. The nucleus is not shown. For simplicity, only one set of chromosome II and IV homologs is shown. Small ovals represent centromeres as designated in Fig. 2. Heavy lines represent chromosome IV, and light lines represent chromosome II. Recombinogenic lesions, such as DSBs, are either generated spontaneously or created by DNA-damaging agents. (Left) In *RAD9*$^+$ strains, DSBs arrest cells in G_2 and trigger SCE, resulting in the repair of the DSB. (Right) In *rad9* mutants, no cell cycle arrest occurs, and centric and acentric chromosomal fragments are inherited in daughter cells after segregation. Recombination between nonhomologs then generates translocations *CEN2*::IV and *CEN4*::II.

that does not generate translocations. Since prearresting cells with nocodazole does not completely suppress the UV sensitivity of *rad9* mutants (1), the inability to completely suppress the *rad9* hyper-Rec phenotype by nocodazole may be correlated with other *rad9* phenotypes, such as the increased activity of the putative 3′-5′ Rad17 nuclease (36). Thus, deficient cell cycle arrest at the G_2 checkpoint is likely to be one of several factors that increase translocation events.

Since the major yeast DSB repair pathway is homologous recombination (46, 64) and one DSB is sufficient to arrest cells at G_2 (8, 50), G_2-M arrest likely facilitates DSB repair by SCE (Fig. 3). It is therefore logical that both X-ray- and HO endonuclease-induced SCE were significantly decreased in *rad9* mutants that cannot arrest at the G_2-M checkpoint. Although there is a correlation between defective recombinational repair of DSBs by SCE and elevated numbers of X-ray-induced translocations, further studies will be necessary to demonstrate cause and effect.

The observation that the frequencies of HO endonuclease-induced translocations were the same in *RAD9*$^+$ and *rad9* diploid mutants is consistent with the idea that sister chromatids are preferred substrates for recombinogenic repair of DSBs. DNA damage caused by environmental agents differs from that caused by site-specific endonucleases in that environmental agents, such as ionizing radiation, would likely create DSBs at nonidentical loci on sister chromatids. Thus, an undamaged sister chromatid may serve as a template for recombinational repair of radiation-induced DNA damage. Since the *HOcs* would be at identical loci on sister chromatids, we speculate that HO endonuclease could cleave both sister chromatids at the same location. Repair of both HO endonuclease-generated DSBs at unique sequences cannot occur by homologous recombination between sister chromatids if there are two identically cleaved chromatids. We suggest that the frequency of HO-induced translocations could not be increased in *rad9* mutants because SCE may not contribute to recombinational repair of the targeted DSB in the *RAD9*$^+$ strain.

Our results indicate that the correlation between increased numbers of DNA damage-induced translocations and decreased numbers of DNA damage-induced SCE in *rad9* mutants depends on the DNA-damaging agent; environmental agents that create DNA DSBs demonstrated the best correlation. *RAD9*-independent SCE may result from (i) DNA lesions that trigger cell cycle arrest at other checkpoints and (ii) recombinational pathways that generate SCE but not translocations. For example, MMS and UV stimulation of SCE may result from DNA lesions that arrest the cell cycle at the S-phase checkpoint (28), which is attenuated but not absent in the *rad9* mutant (43). Since UV can stimulate *RAD1*-independent SCE (28), whereas the *rad9* hyper-Rec phenotype is *RAD1* dependent, there are differences between the UV-induced recombinational pathway(s) that generate SCE and those that generate higher levels of translocations. Thus, although the defective G_2 checkpoint may result in more translocations, some DNA-damaging agents may create lesions that can be repaired by SCE at other cell cycle checkpoints.

Elevated numbers of translocations in *rad9* mutants are generated by a *RAD1*-dependent recombination pathway. Our results indicate that with respect to the *rad9* hyper-Rec phenotype, *RAD1* is epistatic to *RAD9*. Rad1, as part of the Rad1-Rad10 endonuclease that participates in UV excision repair (6), has been suggested to play two different roles in the formation of recombinogenic substrates: first, it processes DNA lesions into DSBs that can initiate mitotic recombination (39), and second, it cleaves nonhomologous DNA from recombinogenic DSBs to form stable recombination intermediates (20). *RAD1*-dependent hyper-Rec phenotypes are found for other mutants, including *top3* (5), *pms1* (4), and *rem* (39) mutants that are defective in Topo3, mismatch repair, and the Rad3 helicase, respectively. Both *top3* and *pms1* mutants exhibit enhanced ectopic recombination between the homologous *SAM1* and *SAM2* genes (4, 5). Thus, gene(s) involved in the excision repair pathway contribute to genomic instability observed in both DNA repair and cell cycle checkpoint mutants.

Chromosomal polymorphisms occur in *rad9* mutants. Chromosomal rearrangements generated in the *rad9* mutant indicate that genetic instability is not limited to directed translocations. It is unknown whether recombinants containing nonreciprocal translocations first contained reciprocal translocations and lost *CEN4*::II or whether the nonreciprocal translocations were generated in the absence of the reciprocal product. The unusual chromosomal polymorphisms present in *rad9* mutants are secondary changes that likely occurred by recombination between dispersed repetitive sequences (22), as has been suggested for naturally occurring chromosome III polymorphisms (72).

Since chromosomal fragments may be passed on from mother cell to daughter cell in *rad9* mutants, it is intriguing to imagine that some nonreciprocal translocations result from recombination of chromosomal fragments that are inherited in subsequent generations but remain recombinogenic. Recombination mechanisms that generate nonreciprocal translocations may be similar to those that generate longer yeast artificial chromosomes. Vollrath et al. (66) observed that in vivo recombination between the free end of a yeast artificial chro-

mosome and the corresponding homologous genomic sequences results in larger artificial linear chromosomes that include DNA sequences from the homologous genomic sequence to the telomere. Similar mechanisms may account for the generation of the DSB-initiated nonreciprocal translocations (Fig. 3).

Our results may seem to contradict observations that mitotic rates of spontaneous, allelic recombination (68) and intrachromosomal recombination between direct repeats (53) are unchanged in *rad9* mutants. After careful examination of previous studies, we offer the following explanations. First, the rate of spontaneous translocations in *rad9* mutants is approximately 10- or 1,000-fold less than the rates of spontaneous allelic or intrachromatid events (ICE) in *RAD9*$^+$, respectively, and thus if the same number of recombinants are stimulated in these assays, enhanced allelic events or ICE may be too few to detect among background events. Second, ICE and allelic recombination assays detect recombination events that are not associated with exchange of flanking markers and occur predominately by deletion (21, 52) and gene conversion (23), respectively, whereas translocations occur by recombination associated with exchange of flanking markers. Because mitotic gene conversion and reciprocal exchange can occur by independent pathways (29) and mutants may be hyper-Rec for one pathway but not the other (2), it may not be surprising that mutations in checkpoint genes may elevate particular types of mitotic recombination.

In summary, the phenotype of *rad9* mutants includes higher mitotic levels of spontaneous and DNA damage-associated translocations. This is the first hyper-Rec phenotype assigned to the *rad9* mutant. Although several factors may contribute to this phenotype, one factor is failure to channel repair of DSBs into SCE. Since additional cell cycle checkpoints have been identified in yeast (71), it will be interesting to determine whether other checkpoint mutants have similar recombination phenotypes.

ACKNOWLEDGMENTS

We especially thank B. Kalemba for excellent secretarial support and P. Dave for technical support when the project was initiated. We thank S. Honigberg, R. Bauchwitz, B. Wilcox, R. Barrington, H. Lieberman, and A. Driks for useful discussions. We thank L. Prakash, D. Schild, and T. Weinert for plasmids used to make *rad1*, *rad52*, and *rad9* disruptions, respectively.

This work was supported by Public Health Service grant CA70105 from the National Cancer Institute and a grant from the Leukemia Research Foundation.

REFERENCES

1. **Aboussekhra, A., J. E. Vialard, D. Morrison, M. A. Torr-Ruiz, L. Cernakova, F. Fabre, and N. F. Lowndes.** 1996. A novel role for the budding yeast *RAD9* checkpoint gene in DNA damage-dependent transcription. EMBO J. **15:** 3912–3933.
2. **Aguilera, A., and H. L. Klein.** 1988. Genetic control of intrachromosomal recombination in *Saccharomyces cerevisiae*. I. Isolation and genetic characterization of hyper-recombination mutants. Genetics **119:**779–790.
3. **Ausubel, F. M., R. Brent, R. E. Kingston, D. D. Moore, J. G. Seidman, J. A. Smith, and K. Struhl (ed.).** 1994. Current protocols in molecular biology. John Wiley & Sons, Inc., New York, N.Y.
4. **Bailis, A. M., and R. Rothstein.** 1990. A defect in mismatch repair in *Saccharomyces cerevisiae* stimulates ectopic recombination between homologous genes by an excision repair process. Genetics **126:**535–547.
5. **Bailis, A. M., L. Arthur, and R. Rothstein.** 1992. Genome rearrangement in *top3* mutants of *Saccharomyces cerevisiae* requires a functional *RAD1* excision repair gene. Mol. Cell. Biol. **12:**4988–4993.
6. **Bardwell, A. J., L. Bardwell, A. E. Tomkinson, and E. C. Friedberg.** 1994. Specific cleavage of model recombination and repair intermediates by the yeast Rad1/Rad10 endonuclease. Science **265:**2082–2085.
7. **Beamish, M., and M. F. Levin.** 1994. Radiosensitivity in ataxia telangiectasia: anomalies in radiation-induction cell cycle delay. Int. J. Radiat. Biol. **65:**175–184.
8. **Bennett, C. B., A. L. Lewis, K. K. Baldwin, and M. A. Resnick.** 1993. Lethality induced by a single site-specific double-strand break in a dispensable yeast plasmid. Proc. Natl. Acad. Sci. USA **90:**5613–5617.
9. **Boeke, J. D., F. Lacroute, and G. R. Fink.** 1984. A positive selection for mutants lacking orotidene-5′-phosphate decarboxylase activity in yeast: 5-fluoro-orotic acid resistance. Mol. Gen. Genet. **197:**345–347.
10. **Brunborg, G., M. Resnick, and D. H. Williamson.** 1980. Cell-cycle-specific repair of DNA DSBs in *Saccharomyces cerevisiae*. Radiat. Res. **82:**547–558.
11. **Brunborg, G., and D. H. Williamson.** 1978. The relevance of the nuclear division cycle to radiosensitivity in yeast. Mol. Gen. Genet. **162:**277–286.
12. **Chen, D., B. Yang, and T. Kuo.** 1992. One-step transformation of yeast in stationary phase. Curr. Genet. **21:**83–84.
13. **Chu, G. D., D. Vollrath, and R. W. Davis.** 1986. Separation of large DNA molecules by contour-clamped homogeneous electric fields. Science **234:** 1582–1585.
14. **Esposito, M. S., D. T. Maleas, K. A. Bjornstad, and C. V. Bruschi.** 1982. Simultaneous detection of changes in chromosome number, gene conversion and intergenic recombination during mitosis of *Saccharomyces cerevisiae*: spontaneous and ultraviolet light induced events. Curr. Genet. **6:**5–11.
15. **Fabre, F., A. Boulet, and H. Roman.** 1984. Gene conversion at different points in the mitotic cycle of *Saccharomyces cerevisiae*. Mol. Gen. Genet. **195:**139–143.
16. **Fasullo, M. T., and R. W. Davis.** 1987. Recombinational substrates designed to study recombination between unique and repetitive sequences *in vivo*. Proc. Natl. Acad. Sci. USA **84:**6215–6219.
17. **Fasullo, M. T., and R. W. Davis.** 1988. Direction of chromosomal rearrangements in the yeast *Saccharomyces cerevisiae* by use of *his3* recombinational substrates. Mol. Cell. Biol. **8:**4370–4380.
18. **Fasullo, M. T., P. Dave, and R. Rothstein.** 1994. DNA-damaging agents stimulate the formation of directed reciprocal translocations in *Saccharomyces cerevisiae*. Mutat. Res. **314:**121–133.
19. **Fasullo, M. T., and P. Dave.** 1994. Mating type regulates the radiation-associated stimulation of reciprocal translocation events in *Saccharomyces cerevisiae*. Mol. Gen. Genet. **243:**63–70.
20. **Fishman-Lobell, J., N. Rudin, and J. E. Haber.** 1992. Removal of nonhomologous DNA ends in double-strand break recombination: the role of the yeast ultraviolet repair gene *RAD1*. Science **258:**480–484.
21. **Galli, A., and R. Schiestl.** 1995. On the mechanism of UV and gamma-ray induced intrachromosomal recombination in yeast cells synchronized in different stages of the cell cycle. Mol. Gen. Genet. **248:**301–310.
22. **Goffeau, A., B. G. Barrell, H. Bussey, R. W. Davis, B. Dujon, J. Feldmann, F. Galibert, J. D. Hoheisel, C. Jacq, M. Johnston, E. J. Louis, H. W. Mewes, Y. Murakami, P. Philippsen, H. Tettelin, and S. G. Oliver.** 1996. Life with 6000 genes. Science **274:**546–567.
23. **Golin, J. E., and M. S. Esposito.** 1981. Mitotic recombination: mismatch correction and replicational resolution for Holliday structures formed at the two-strand stage in *Saccharomyces cerevisiae*. Mol. Gen. Genet. **183:**252–253.
24. **Higgins, D. R., S. Prakash, P. Reynolds, and L. Prakash.** 1983. Molecular cloning and characterization of the *RAD1* gene of *Saccharomyces cerevisiae*. Gene **26:**119–126.
25. **Jacobs, C., A. Adams, P. Szanszlo, and J. Pringle.** 1988. Functions of microtubules in the *Saccharomyces cerevisiae* cell cycle. J. Cell Biol. **107:**1409–1426.
26. **Jensen, R., and I. Herskowitz.** 1984. Directionality and regulation of cassette substitution in yeast. Cold Spring Harbor Symp. Quant. Biol. **49:**13–21.
27. **Kadyk, L. C., and L. H. Hartwell.** 1992. Sister chromatids are preferred over homologs as substrates for recombinational repair in *Saccharomyces cerevisiae*. Genetics **132:**387–402.
28. **Kadyk, L. C., and L. H. Hartwell.** 1993. Replication dependent sister chromatid recombination in *rad1* mutants of *Saccharomyces cerevisiae*. Genetics **133:**469–487.
29. **Klein, H. L.** 1984. Lack of association of intrachromosomal gene conversion and reciprocal exchange. Nature **310:**748–753.
30. **Kostriken, R., and F. Heffron.** 1984. The product of the *HO* gene is a nuclease: purification and characterization of the enzyme. Cold Spring Harbor Symp. Quant. Biol. **49:**89–104.
31. **Kupiec, M., and G. Simchen.** 1985. Arrest of the mitotic cell cycle and of meiosis in *Saccharomyces cerevisiae* by MMS. Mol. Gen. Genet. **201:**558–564.
32. **Lawrence, C. W., and R. Christiansen.** 1976. UV mutagenesis in radiation sensitive strains of yeast. Genetics **82:**207–232.
33. **Lea, D. E., and C. A. Coulson.** 1949. The distribution of the numbers of mutants in bacterial populations. J. Genet. **49:**264–284.
34. **Lesser, C., and C. Guthrie.** 1993. Mutational analysis of pre-mRNA splicing in *Saccharomyces cerevisiae* using a sensitive new reporter gene, *CUP1*. Genetics **133:**851–863.
35. **Livingston, K. R., A. White, J. Sprouse, E. Livanos, T. Jacks, and T. Tisty.** 1992. Altered cell cycle arrest and gene amplification potential accompany loss of wild-type p53. Cell **70:**923–935.
36. **Lydall, D., and T. Weinert.** 1995. Yeast checkpoint genes in DNA damage processing: implications for repair and arrest. Science **270:**1488–1491.
37. **Metcalfe, J. A., A. Heppell-Parton, C. M. McConville, and A. M. Taylor.** 1991. Characterization of a B-lymphocyte t(2;14) (p11;q32) translocation

from an ataxia telangiectasia patient conferring a proliferative advantage on cells in vitro. Cytogenet. Cell Genet. **56:**91–98.
38. **Meyn, M. S.** High spontaneous intrachromosomal recombination rates in ataxia-telangiectasia. Science **260:**1327–1330.
39. **Montelone, B. A., M. F. Hoekstra, and R. E. Malone.** 1988. Spontaneous mitotic recombination in yeast: the hyper-recombinational *rem1* mutations are alleles of the *RAD3* gene. Genetics **119:**289–301.
40. **Nickoloff, J. A., E. Y. Chen, and F. Heffron.** 1986. A 24-base-pair DNA sequence from the MAT locus stimulates intergenic recombination in yeast. Proc. Natl. Acad. Sci. USA **83:**7831–7835.
41. **Pandita, T. K., S. Pathak, C. R. Geard.** 1995. Chromosome end associations, telomeres, and telomerase activity in ataxia telangiectasia. Cytogenet. Cell Genet. **71:**86–93.
42. **Parket, A., O. Inbar, and M. Kupiec.** 1995. Recombination of Ty elements in yeast can be induced by a double-strand break. Genetics **140:**67–77.
43. **Paulovich, A. G., R. U. Margulies, B. M. Garvick, and L. H. Hartwell.** 1997. *RAD9*, *RAD17*, and *RAD24* are required for S phase regulation in *Saccharomyces cerevisiae* in response to DNA damage. Genetics **145:**45–62.
44. **Paulovich, A. G., C. D. Armour, and L. H. Hartwell.** 1997. Unpublished data.
45. **Rattray, A. J., and L. S. Symington.** 1995. Multiple pathways for homologous recombination in *Saccharomyces cerevisiae*. Genetics **139:**45–56.
46. **Resnick, M. A., and P. Martin.** 1976. The repair of DSBs in the nuclear DNA of *Saccharomyces cerevisiae* and its nuclear control. Mol. Gen. Genet. **143:** 119–129.
47. **Roman, H., and F. Fabre.** 1983. Gene conversion and associated reciprocal recombination are separable events in vegetative cells of *Saccharomyces cerevisiae*. Proc. Natl. Acad. Sci. USA **80:**6912–6916.
48. **Rothstein, R. J.** 1983. One-step gene disruption in yeast. Methods Enzymol. **101:**202–211.
49. **Rudolph, N. S., and S. A. Latt.** 1989. Flow cytometric analysis of X-ray sensitivity in ataxia telangiectasia. Mutat. Res. **211:**31–41.
50. **Sandell, L., and V. Zakian.** 1993. Loss of a yeast telomere: arrest, recovery and chromosome loss. Cell **75:**729–739.
51. **Scherer, S., and R. W. Davis.** 1979. Replacement of chromosome segments with altered DNA sequences *in vitro*. Proc. Natl. Acad. Sci. USA **76:**491–495.
52. **Schiestl, R. H., and S. Prakash.** 1988. *RAD1*, an excision repair gene of *Saccharomyces cerevisiae*, is also involved in recombination. Mol. Cell. Biol. **8:**3619–3626.
53. **Schiestl, R. H., P. Reynolds, S. Prakash, and L. Prakash.** 1989. Cloning and sequence analysis of the *Saccharomyces cerevisiae RAD9* gene and further evidence that its product is required for cell cycle arrest induced by DNA damage. Mol. Cell. Biol. **9:**1882–1896.
54. **Schiestl, R. H.** 1989. Nonmutagenic carcinogens induce intrachromosomal recombination in yeast. Nature **337:**285–288.
55. **Schild, D., I. L. Calderon, R. Contopoulou, and R. K. Mortimer.** 1983. Cloning of yeast recombination repair genes and evidence that several are non-essential genes, p. 417–427. *In* E. C. Friedberg and B. A. Bridges (ed.), Cellular responses to DNA damage. Alan R. Liss Inc., New York, N.Y.
56. **Schwartz, D., and C. Cantor.** 1984. Separation of yeast chromosome-sized DNAs by pulse field gradient gel electrophoresis. Cell **37:**67–75.
57. **Sherman, F., G. R. Fink, and J. B. Hicks.** 1982. Methods of yeast genetics. Cold Spring Harbor Laboratory, Cold Spring Harbor, N.Y.
58. **Siede, W., A. S. Friedberg, and E. C. Friedberg.** 1993. *RAD9*-dependent G_1 arrest defines a second checkpoint for damaged DNA in the cell cycle of *Saccharomyces cerevisiae*. Proc. Natl. Acad. Sci. USA **90:**7985–7989.
59. **Siede, W., A. S. Friedberg, I. Dianova, and E. C. Friedberg.** 1994. Characterization of G_1 checkpoint control in the yeast *Saccharomyces cerevisiae* following exposure to DNA-damaging agents. Genetics **138:**271–281.
60. **Southern, E. M.** 1975. Detection of specific sequences among DNA fragments separated by gel electrophoresis. J. Mol. Biol. **98:**503–517.
61. **Stinchcomb, S., C. Mann, and R. W. Davis.** 1982. Centromeric DNA from *Saccharomyces cerevisiae*. J. Mol. Biol. **158:**157–179.
62. **Struhl, K., and R. W. Davis.** 1980. A physical, genetic, and transcriptional map of the cloned *his3* gene region of *Saccharomyces cerevisiae*. J. Mol. Biol. **136:**309–332.
63. **Struhl, K.** 1985. Nucleotide sequence and transcriptional mapping of the yeast *PET56-HIS3-DED1* gene region. Nucleic Acids Res. **13:**8585–8601.
64. **Szostak, J. W., T. L. Orr-Weaver, R. Rothstein, and F. W. Stahl.** 1983. The double-strand break model for recombination. Cell **33:**25–35.
65. **Torchia, E., and J. E. Hopper.** 1986. Genetic and molecular analysis of the *GAL3* gene in the expression of the galactose/melibiose regulon of *Saccharomyces cerevisiae*. Genetics **113:**229–246.
66. **Vollrath, D., R. W. Davis, C. Connelly, and P. H. Hieter.** 1988. Physical mapping of large DNA by chromosome fragmentation. Proc. Natl. Acad. Sci. USA **85:**6027–6031.
67. **Weinert, T., and L. H. Hartwell.** 1988. The *RAD9* gene controls the cell cycle response to DNA damage in *Saccharomyces cerevisiae*. Science **241:**317–322.
68. **Weinert, T., and D. Lydall.** 1993. Cell cycle checkpoints, genetic instability and cancer. Semin. Cancer Biol. **4:**129–140.
69. **Weinert, T. A., and L. H. Hartwell.** 1990. Characterization of the *RAD9* gene of *Saccharomyces cerevisiae* and evidence that it acts posttranslationally in cell cycle arrest after DNA damage. Mol. Cell. Biol. **10:**6554–6564.
70. **Weinert, T. A., and L. H. Hartwell.** 1993. Cell cycle arrest of *cdc* mutants and specificity of the *RAD9* checkpoint. Genetics **134:**63–80.
71. **Weinert, T. A., G. L. Kiser, and L. H. Hartwell.** 1994. Mitotic checkpoint genes in budding yeast and the dependence of mitosis on DNA replication and repair. Genes Dev. **8:**652–665.
72. **Wicksteed, B. L., I. Collins, K. A. Dershowitz, L. I. Stateva, R. P. Green, S. G. Olvier, A. J. Brown, and C. S. Newlon.** 1994. A physical comparison of chromosome III in six strains of *Saccharomyces cerevisiae*. Yeast **10:**39–57.
73. **Yin, Y., M. A. Tainsky, F. Z. Bischoff, L. C. Strong, and G. M. Wahl.** 1992. Wild-type p53 restores cell cycle control and inhibits gene amplification in cells with mutant p53 alleles. Cell **70:**937–948.
74. **Zar, J. H.** 1984. Biostatistical analysis. Prentice Hall, Inc., Englewood Cliffs, N.J.